British Journal of Pharmacology (2007) 152, 161–167
 0007–1188/07 $30.00
www.brjpharmacol.org

RESEARCH PAPER

Intraglandular application of botulinum toxin leads to structural and functional changes in rat acinar cells

A Teymoortash[1], F Sommer[1], R Mandic[1], S Schulz[2], M Bette[3], G Aumüller[3] and JA Werner[1]

[1]*Department of Otolaryngology, Head and Neck Surgery, Philipp University, Marburg, Germany;* [2]*Department of Veterinary Services, Philipp University, Marburg, Germany and* [3]*Institute of Anatomy and Cell Biology, Philipp University, Marburg, Germany*

Background and purpose: Intraglandular injection of botulinum toxin (BoNT) leads to a transient denervation of the submandibular gland and this is associated with reduced salivary secretion. The purpose of the present study was to verify whether temporary acinar atrophy occurs simultaneously with chemical denervation of the glands.
Experimental approach: Tissue specimens of the right submandibular gland taken from 18 Wistar rats after intraglandular injection of BoNT A, BoNT B, or a combination of both were examined. As a sham control, an equivalent volume of saline was injected into the left submandibular gland. Morphometric measurements, immunohistochemistry, electron microscopy and western blot analysis were used to analyse the morphological and functional changes of the denervated glands.
Key results: Morphological and ultrastructural analyses of the cell organelles and secretory granula showed a clear atrophy of the acini, which was more prominent in glands injected with the combination of BoNT/A and B. Morphometric measurements of the glandular acini revealed a significant reduction of the area of the acinar cells after injection of BoNT ($P = 0.031$). The expression of amylase was significantly reduced in BoNT treated glands.
Conclusions and implications: Intraglandular application of BoNT induces structural and functional changes of the salivary glands indicated by glandular atrophy. These effects may be due to glandular denervation induced by the inhibition of the soluble *N*-ethylmaleimide-sensitive fusion protein attachment protein receptors (SNAREs) involved in acetylcholine release at the neuroglandular junction and also specially inhibition of those involved in exocytosis of the granula of the acinar cells.
British Journal of Pharmacology (2007) **152,** 161–167; doi:10.1038/sj.bjp.0707375; published online 9 July 2007

Keywords: botulinum toxin; acinar atrophy; structural changes; electron microscopy; amylase expression

Abbreviations: BoNT, botulinum toxin; SNAP, synaptosomal-associated protein; SNAREs, soluble *N*-ethylmaleimide-sensitive fusion protein attachment protein receptors; VAMP, vesicle-associated membrane protein, synaptobrevin

Introduction

The autonomic nervous system regulates the salivary protein and fluid secretion. These nerves often exhibit similar effects on salivary secretory cells and myoepithelial cells (Garrett, 1987) . Electrical stimulation of the innervating parasympathetic nerve in rats induces a considerable flow of saliva with low protein content (Garrett *et al*., 1991). Stimulation of muscarinic receptors enhances the cytosolic Ca^{2+} concentration and induces a relatively limited release of amylase (Yoshimura *et al*., 2002), whereas sympathetic impulses cause exocytosis of acinar granules but little fluid secretion. The accumulation of cAMP following the stimulation of β-adrenoceptors activates cAMP-dependent protein kinase, resulting in a high level of amylase release (Fujita-Yoshigaki, 1998).

Drooling is common in patients with neurological disorders such as amyotrophic lateral sclerosis, Parkinson's disease and cerebral palsy. Application of botulinum toxin (BoNT) has been shown to be effective in the treatment of hypersalivation accompanying various diseases (Lipp *et al*., 2003; Jongerius *et al*., 2004). Pharmacological denervation of the salivary glands by intraglandular application of BoNT causes inhibition of acetylcholine release at the neuroglandular junction (chemical parasympathectomy) and produces a distinct reduction in salivary flow. Simultaneously, an increase in the concentration of salivary components can be observed (Ellies *et al*., 2002). However, when this concentration was calculated on the basis of flow rate per minute no significant difference between the protein concentration in the output before and after BoNT application was revealed. On the basis of studies in rats and humans, these effects are explained by the dual innervation

Correspondence: Dr A Teymoortash, Department of Otolaryngology, Head and Neck Surgery, Philipp University, Deutschhausstr. 3, Marburg 35037, Germany.
E-mail: teymoort@med.uni-marburg.de
Received 21 May 2007; accepted 8 June 2007; published online 9 July 2007

of the salivary glands. BoNT selectively inhibits the cholinergic components but the adrenergic innervation is left mainly intact (Ellies *et al*., 2004). However, the precise effects of an intraglandular injection of BoNT on salivary protein production and function of the salivary glands cannot be determined from these existing data.

Morphometric studies of the rat submandibular gland after BoNT/A treatment demonstrated no significant difference between toxin- and saline-injected glands (Ellies *et al*., 1999). But the morphometric evaluations in this study were limited to descriptions of nuclei of the serous acinar cells. In addition, these authors did not use a standardized fixation method to minimize differences in the shrinkage of the tissue samples. Hence, the aim of the present study was to analyse the direct effect of locally injected BoNT/A and B on the precise morphological changes in the submandibular gland at the cellular and ultrastructural level. The results should help to elucidate the biological effects of these toxins on salivary glands.

Methods

Animals and injections

Eighteen adult male Wistar rats weighing 250–300 g were used. The animals were housed in the animal care centre under controlled light and environmental conditions (12:12 h dark/light cycle; $23 \pm 1^{\circ}C$; 55% relative humidity). Food and water were available *ad libitum*. The animals were monitored for behaviour, food and water intake, and body weight was measured daily. All experiments were performed between 1400 and 1600 hours. Subsequent experiments were approved by the University Animal Care Committee.

Anaesthesia was induced by an intramuscular injection of $100\,mg\,kg^{-1}$ ketamine in combination with $5\,mg\,kg^{-1}$ xylazine. The toxin was applied to the submandibular gland via a horizontal neck incision or the animal was sham treated on both sides. In each animal, the right submandibular gland was treated once with the toxin and the left submandibular gland of the same rat was used as the internal sham control. The BoNT-treated rats were divided into three different groups (six rats per group): BoNT/A, received an injection of 5 U BoNT/A in 0.1 ml saline; BoNT/B, injected with 250 U BoNT/B (1:50, conversion factor) in 0.1 ml saline; BoNT/AB, injected with a mixture of both BoNT/A (5 U) and BoNT/B (250 U). The sham group was treated with saline in a similar manner. On day 14, the rats were anaesthetized as mentioned above and killed by cardiac puncture with T61. The submandibular glands were dissected from the surrounding connective tissue and removed. From each gland, tissue samples were preserved for studying their histology and immunochemistry, as well as for electron microscopy and western blot analysis.

Bright-field microscopy

For bright-field microscopy, a sample of the fresh glandular tissue was immersed overnight in Bouin Hollande fixative. After fixation, the tissue was extensively washed in 70% 2-propanol and processed for routine paraffin embedding. These steps were performed synchronously as an automatic procedure (Tissue Tek VIP) for standard fixation of all samples and to prevent inhomogeneous shrinkage of the samples for morphometric studies.

Morphometric studies were carried out in serous acini of haematoxylin and eosin-stained sections. The area of one acinar cell was calculated by measuring the area occupied by all the cells in an acinus and dividing this result by the number of acinar cells in that acinus. To obtain the mean values of the data, 25 records per sample from each gland were analysed in randomly selected microscopic fields and measured by digital imaging. The sections were digitized with an Olympus AX-70 microscope and morphometric measurements were obtained by using the MCID Image Analyze System.

Immunohistochemical staining for amylase was carried out by the avidin–biotin–peroxidase complex (ABC) method, using a commercially available kit (DAKO Cytomation, Glostrup, Denmark). Briefly, deparaffinized and rehydrated sections (3–5 μm) were incubated with $0.01\,mol\,l^{-1}$ citrate buffer (pH 6.0) three times for 5 min in a household 700-W microwave oven. After the microwave antigen retrieval, the sections were allowed to cool down to room temperature and washed with Tris-buffered saline (TBS). All the sections were treated with methanol containing 1% H_2O_2 for 10 min. After washing in phosphate-buffered saline (PBS), normal rabbit serum was applied for 20 min. Then, the primary antibody reacted at 4°C overnight in a dilution of 1:100 for anti-amylase polyclonal antibody. After washing in PBS, biotinylated, affinity-purified antigoat IgG was applied for 30 min as a secondary antibody, followed by peroxidase-marked avidin–biotin complex for 30 min. Peroxidase was visualized by ammonium nickel sulphate-enhanced 3,3-diaminobenzidine (DAB) reactions. Haemalaun was used for counterstaining. The staining intensity was graded by two independent observers: (−) absent, (+) low, (++) moderate and (+++) strong.

Electron microscopy

For electron microscopy, glands were cut into small fragments that were immersed in the fixative (2.5% glutaraldehyde, 2.5% paraformaldehyde, 0.5% picric acid in sodium cacodylate buffer, 0.1 M, pH 7.3) (Ito and Karnovsky, 1968). They were then minced into smaller fragments and additionally fixed for about 24 h at room temperature. Following fixation, tissue fragments were washed in sodium cacodylate buffer (0.1 M, pH 7.3) three times, and treated for 1 h with reduced osmium tetroxide solution (Karnovsky, 1971). After careful washings in sodium cacodylate buffer, tissue fragments were dehydrated in a graded series of ethanols, propylene oxide and soaked with epon resin diluted in propylene oxide, followed by overnight penetration with full epon resin mixture. Samples were filled into gelatine capsules, covered with epon mixture and polymerization was performed for 24 h at 60°C. Blocks were trimmed and semi-thin sections were cut with a glass knife on a Reichert ultramicrotome, mounted on glass slides, and stained with toluidine blue–pyronin in borax solution for histological studies (Ito and Winchester, 1963). Appropriate areas were

selected from the blocks and were cut with a diamond knife on a Reichert ultramicrotome. Ultra-thin sections were collected on 100-mesh copper grids and stained with lead citrate and uranyl acetate (Venable and Coggeshall, 1965). Sections were then examined in a Zeiss EM 10C electron microscope (Zeiss, Jena, Germany).

Western blot studies

Expression of amylase was evaluated by western blot analysis. The glandular tissue was minced into small pieces and suspended in lysis buffer (1% NP-40, 66 mM EDTA, 10 mM Tris–HCl). Forty micrograms of each sample were electrophoretically separated on a 12% SDS–PAGE gel, and then transferred to a nitrocellulose membrane. The membranes were blocked with 3% milk/PBS to prevent nonspecific binding of the antibody and then incubated with amylase antibody (dilution 1:300). This antibody was detected by an ECL kit according to the manufacturer's instructions.

Statistics

All statistical tests were carried out using SPSS (Version 11.5, SPSS Inc., Chicago, IL, USA). The Wilcoxon rank test was used to verify significant differences between the BoNT and saline groups. Differences between the BoNT subgroups were compared with the Kruskal–Wallis test and the Mann–Whitney test. P-values $\leqslant 0.05$ were considered to indicate statistical significance.

Materials

Ketamine (Ketavet; Alverta & Werfft AG, Neumünster, Germany), xalazine (Rompun; Bayer Health Care, Leverkusen, Germany), BoNT/A (Botox; Allergan, Westport, Ireland), BoNT/B (NeuroBloc; Solstice Neurosciences, Dublin, Ireland), T61 (Intervet, Unterschleißheim, Germany), ammonium nickel sulphate-enhanced 3,3-diaminobenzidine (DAKO Cytomation, Glostrup, Denmark), anti-amylase polyclonal antibody (Santa Cruz Biotechnology, Inc., Santa Cruz, CA, USA). Tissue Tek VIP (Vogel, Giessen, Germany), MCID Image Analyze System (Imaging Research Inc., St Cathrines, Ontario, Canada) and ECL kit (Amersham Biosciences, Freiburg, Germany).

Results

Glandular weight analysis

Significant decreases in glandular weight occurred after injection with BoNT ($P = 0.004$). The mean reduction of the glandular weight was 29.9 mg (9.2%). Comparison of the glands which were treated with BoNT/B or a combination of BoNT/A and B with glands only treated with BoNT/A revealed a significantly enhanced reduction in glandular weight in those that had received BoNT/B ($P = 0.032$; Figure 1).

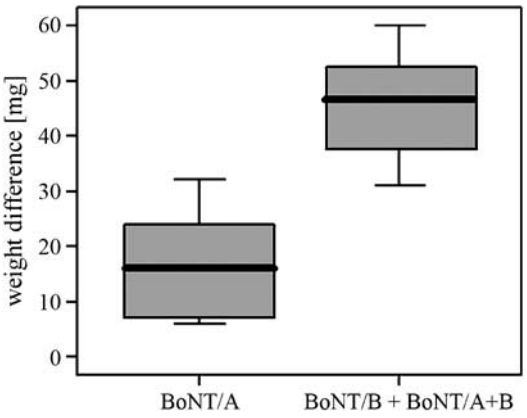

Figure 1 Weight differences between BoNT-injected submandibular glands and sham-injected contralateral submandibular glands. Mean values ± s.d. of BoNT/A and BoNT/B plus BoNT/A + B are shown ($n = 18$). BoNT, botulinum toxin.

Histological analysis

The submandibular gland of control animals typically exhibited a regular appearance with numerous round acini containing an abundance of clear secretory vacuoles; these were surrounded by thin areas of connective tissue containing nerves and vessels. Only a few intercalated ducts with narrow lumen and sparse, darkly stained secretory cells were found, whereas granulated striated ducts with densely packed granules were prominent (Figure 2a).

In BoNT/A- or BoNT/B-treated animals, acini appeared to be packed more densely. Their shape was slightly elongated and the basal basophilic area containing the nucleus was more pronounced at the expense of secretory material. The lumen of the granular striated ducts was wider than in the controls (Figures 2b and c).

Significant changes were seen in glands removed from animals that had received simultaneous administration of BoNT/A and BoNT/B (Figure 2d). There were only a few secretory active acini left surrounded by loosely arranged, cell-rich connective tissue. Several elongated duct-like structures were found with patent lumen surrounded by epithelial cells of a different height and density. Some of them contained dark secretory granules and were indistinguishable from granular striated duct cells. However, most cells did not contain secretory granules. Sometimes, clear cells were seen in the basal region, resembling swollen myoepithelial cells. Generally, the gland showed clear-cut signs of atrophy.

Morphometric analysis

The results obtained from morphometric evaluations indicated that the area of the acinar cells were smaller in rats treated with BoNT than controls (Table 1). We found a significantly smaller area occupied by each individual acinar cell within the BoNT groups ($P = 0.031$). A significant difference between the BoNT subtypes could not be evaluated because of the small number of samples.

Amylase expression

Moderate to strong staining of amylase was present in the cytoplasm of the acinar cells of controls, which was diffuse

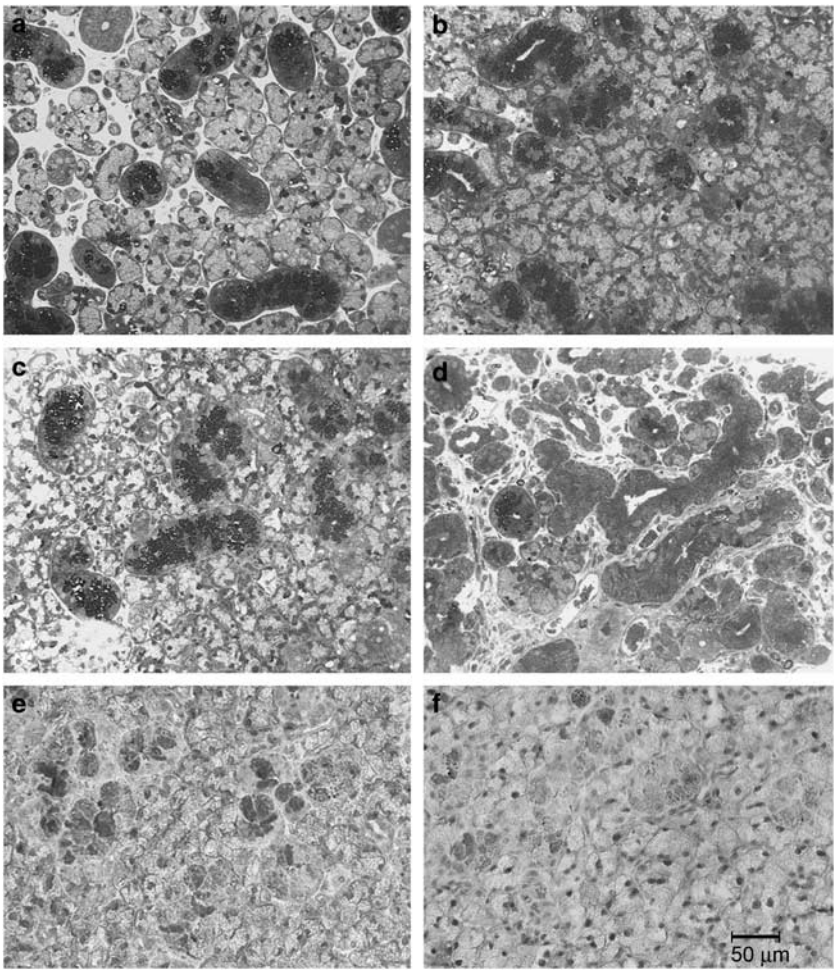

Figure 2 Morphological changes in semi-thin sections of submandibular gland after BoNT application. Sham (**a**) treated with saline, (**b**) treated with BoNT/A, (**c**) treated with BoNT/B, (**d**) treated with BoNT/A + B. (**e** and **f**) Represent amylase expression in 5 μm thin tissue sections of submandibular gland treated with either saline (**e**) or BoNT/B (**f**). Magnification, $\times$40. BoNT, botulinum toxin.

Table 1 Morphometric measurements of serous acini and acinar cells of submandibular glands after injection of BoNT/A, BoNT/B and BoNT/A + B or sham treatment (saline)

Rat number	*Submandibular gland*	*Injection*	*Total acinar area (μm^2)*	*Acinar cell number*	*Area of a single acinar cell (μm^2)*
1	Left	Saline	7995 ± 2066.9	4.6 ± 0.8	1732.5 ± 327.4
	Right	BoNT/A	7134 ± 2071.3	5.0 ± 1.1	1419.9 ± 233.4
2	Left	Saline	6947 ± 1779.1	5.2 ± 1.2	1331.8 ± 144.3
	Right	BoNT/A	6828 ± 1602.5	5.8 ± 1.2	1173.9 ± 102.1
3	Left	Saline	8057 ± 1496.8	4.6 ± 0.8	1751.4 ± 222.4
	Right	BoNT/B	6767 ± 1152.2	4.9 ± 0.7	1376.9 ± 136.7
4	Left	Saline	7446 ± 1743.5	4.9 ± 1.1	1511.7 ± 143.3
	Right	BoNT/B	5506 ± 1331.9	4.6 ± 0.9	1208 ± 147.4
5	Left	Saline	6803 ± 2015.5	4.6 ± 1.0	1478.5 ± 211.3
	Right	BoNT/A + BoNT/B	6923 ± 1867.4	5.7 ± 1.3	1203.9 ± 112.1
6	Left	Saline	7318 ± 1618.6	5.8 ± 1.3	1267 ± 133.7
	Right	BoNT/A + BoNT/B	5761 ± 1230.2	5.0 ± 1.2	1173.1 ± 92.4

Abbreviation: BoNT, botulinum toxin.Each rat received BoNT injection into the right and sham injection into the left submandibular gland. Mean values ± s.d. (n = 6 rats) are given.

and often of variable intensity. Staining intensity in glands treated with BoNT was clearly less when compared to controls. Figures 2e and f shows representative differences in amylase expression in acinar cells between BoNT-treated and control rats.

In accordance with the immunohistochemical results, western blot analysis revealed prominent immunoreactive bands specific for amylase in controls, whereas in submandibular glands treated with BoNT, little or no amylase could be detected (Figure 3).

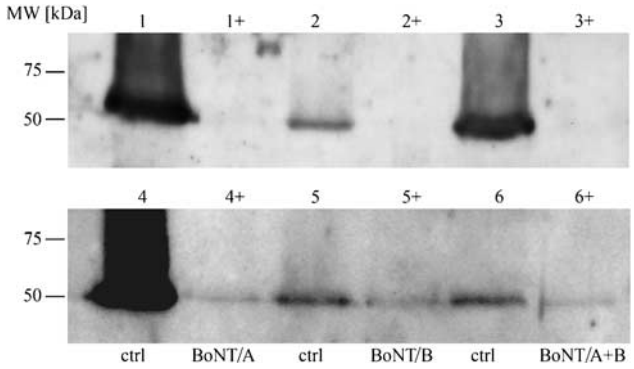

Figure 3 Western blot analysis of the presence of amylase in submandibular glands from six rats. The expression of amylase in the glands treated with BoNT (right gland) was compared with those treated with saline (left gland) from the same rat at the time of death. Lanes 1 to 6 show the presence of amylase in sham-injected control glands (crtl). Lanes 1 + to 6 + show the reduced amount of amylase in glands treated with the different combinations of BoNT. BoNT, botulinum toxin.

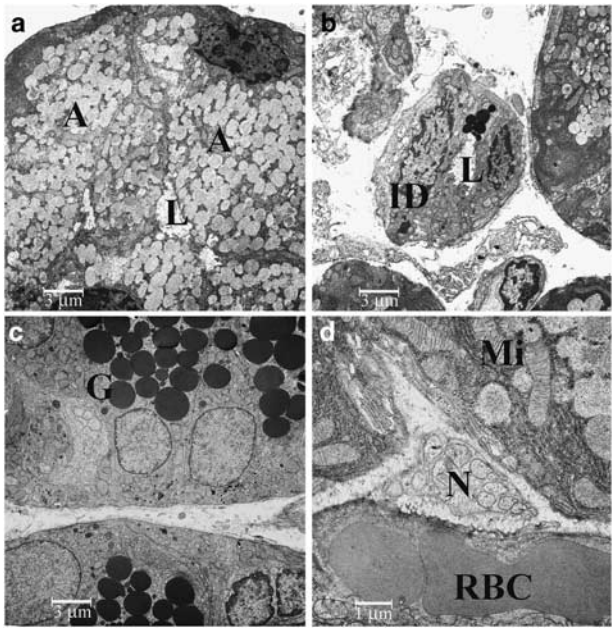

Figure 4 Electron microscopy of glandular tissues from a saline-injected gland: (**a**) acinar cells, ×2710; (**b**) intercalated duct, ×2710; (**c**) granular striated duct, ×2710; (**d**) Schwann cell with terminal axons, ×8750. Abbreviations: A, acinar cell; BoNT, botulinum toxin; G, granula; ID, intercalated duct; L, lumen; Mi, mitochondria; RBC, red blood cells; N, nerve.

Electron microscopy

Acinar secretory cells of control animals (Figure 4a) were replete with secretory vacuoles, containing finely stippled dust-like material. Granules were of homogeneous size and did not coalesce. In the basal compartment, the nucleus was visible, surrounded by rough endoplasmic reticulum and few cytoplasmic organelles were observed. The intercalated ducts contained only a few granular cells (Figure 4b), whereas the latter were abundant in the granular striated ducts. Granular cells (Figure 4c) also contained basally located mitochondria and a small amount of glycogen. Within the interstitial

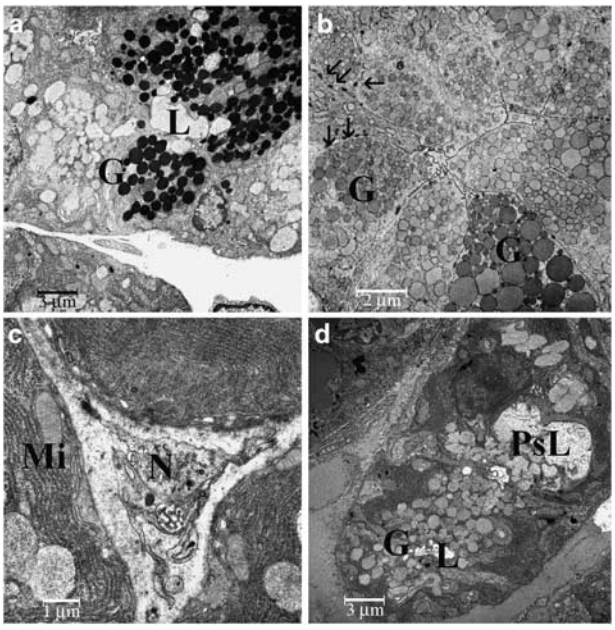

Figure 5 Electron microscopy of glandular tissues from the BoNT groups: (**a**) granular striated duct, BoNT/A, ×2710; (**b**) striated granular cells, BoNT/A, ×3460; (**c**) slightly altered nerve axons, BoNT/A, ×8750; (**d**) acinar cells, BoNT/B, ×2710. Abbreviations: BoNT, botulinum toxin; G, granula; L; lumen; Mi, mitochondria; N, nerve; PsL, pseudolumen. Arrows in (**b**) point to desmosomes.

connective tissue, capillaries and terminal axons of non-myelinated nerves (Figure 4d) were seen, containing mostly small, clear vacuoles, very few small dense-core granules and exceptionally large oval dense-core granules.

Secretory cells in acini from animals that were treated with BoNT/A clearly contained less secretory material. The basally located rough endoplasmic reticulum had increased in size, showing several profiles, intermingled with mitochondria. The structure of the secretory vacuoles appeared altered: there were differences both in size and in electron density. Sometimes, coalescence of secretory vacuoles, forming larger ovoid or polymorphic entities, was seen. On the other hand, interstitial tissue had increased in amount and density. Intercalated ducts contained several secretory cells and cells resembling those of the granular striated duct (Figure 5a). Their lumen was wide and had an irregular shape. In the granular striated ducts, the amount of basal cytoplasm with dense flakes of glycogen, several mitochondria and a few lipofuscin granules had increased. The granules were densely packed, but often appeared less dense than those seen in the controls (Figure 5b). There were considerable differences in the size of the granules, a smaller proportion having significantly increased. In the interstitial nerve axons (Figure 5c), the number of small clear granules was reduced and some dense-core granules of a different size were seen.

There were no major differences with the findings from glands that had been treated with BoNT/B. Acini were small (Figure 5d), with increased amount of rough endoplasmic reticulum, fewer secretory vacuoles of different size and shape and a higher density of interstitial tissue. In intercalated ducts and granular striated ducts, several

desmosomes were seen along with complex interdigitations of adjacent cells.

As already observed in under light microscopy, cellular changes were most noticeable in glands taken from animals treated with both BoNT/A und BoNT/B simultaneously. There were clearly fewer acini with generally reduced size. Even though some of them were replete with relatively large granules containing dust-like material of relatively high electron density, cells appeared shrunken and the cytoplasmic organelles were reduced in number (Figure 6a). Often, the nucleus had a slightly irregular shape with several indentations and finely dispersed chromatin. In place of typical thin intercalated ducts, elongated, curved and thick ducts were found morphologically in-between acini, intercalated ducts and granular striated ducts (Figure 6b). They contained a wide polymorphic lumen and their cells contained both dark round to polymorphic or clear confluent vacuoles, along with several small clear vesicles close to the apical plasma membrane. The typical granular striated ducts had less dark granules, their size and electron density varied considerably (Figure 6c). Basally, the cells contained several densely packed mitochondria and glycogen. In other ducts, granules were very large and were interspersed with a plethora of small vacuole-like granules (Figures 6d and e). The small nerve axons observed inside the Schwann cells (Figure 6f) sometimes contained only a few clear vesicles, whereas adjacent axons had a normal appearance and numbers of vesicles.

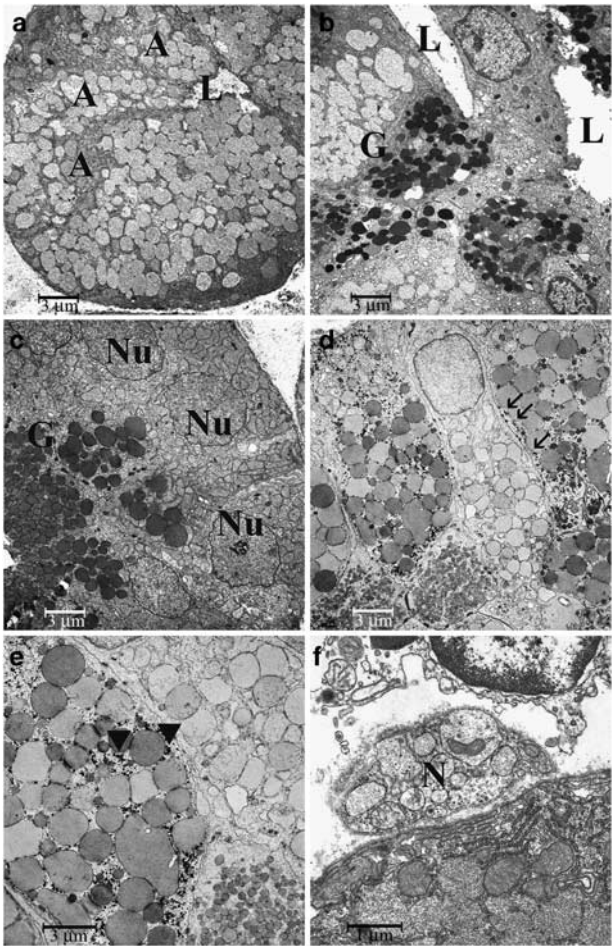

Figure 6 Electron microscopy of glandular samples from the group treated with BoNT/A in combination with BoNT/B: (**a**) acinar cells, ×2710; (**b**) intercalated duct adjacent to an acinar cell, ×2710; (**c** and **d**) striated granular cell, ×2710; (**e**) striated granular cells, ×5450; (**f**) nerve, ×11100. Abbreviations: A, acinar cell; BoNT, botulinum toxin; G, granula; L, lumen; Mi, mitochondria; N, nerve; Nu, nucleus. Arrows in (**d**) point to desmosomes, arrow heads in (**e**) point to glycogen emplacements.

Discussion

Parasympathetic nerves exert a trophic effect on salivary glands. Parasympathetic denervation by sectioning of the chorda tympani in rats produced a decrease in the weight of the submandibular gland, by between 15 and 30%, and caused the acinar cells to shrink (Schneyer and Hall, 1966; Ekstrom and Reinhold, 2001). The DNA content per gland was not reduced after denervation indicating that cell death had not occurred in glandular cells (Poat and Templeton, 1982). These changes cannot be attributed solely to a loss of acetylcholine. The mechanisms underlying the effects of denervation are still not understood.

The ultrastructural studies after intraglandular application of BoNT in the present study showed clear signs of atrophy of the glandular cells, with reduced amounts of granula in the acinar cells, which were smaller in size, polymorph and appeared less electron dense in comparison to the controls. On the basis of the morphological and ultrastructural observations, nuclear apoptotic changes were not observed in the samples studied. The reduction in the weight of the submandibular gland, of 9.2% after treatment with BoNT, observed in the present study is compatible with these results. In the groups that were also injected with BoNT/B, the weight of this gland was significantly reduced in comparison with that from the BoNT/A group.

The morphometric evaluations indicated that the acinar cells were significantly smaller in rats treated with BoNT than in the controls. These measurements confirmed the structural findings. The reduced expression of amylase in immunohistochemical and western blot analysis revealed functional glandular changes after application of BoNT.

BoNT/A cleaves SNAP-23(25) (synaptosomal-associated protein) and BoNT/B VAMP (vesicle-associated membrane protein, synaptobrevin), enzymes involved in the release of acetylcholine at the presynaptic membrane of parasympathetic nerves. In this way, a temporary chemical denervation of the target organ is established. The exocytosis in exocrine cells depends also on SNAREs (soluble *N*-ethylmaleimide-sensitive fusion protein attachment protein receptors) (Fujita-Yoshigaki *et al*., 1999; Nashida *et al*., 2006). In salivary gland acinar cells, VAMP-2 has been found on secretory granule membranes (Fujita-Yoshigaki *et al*., 1996). In parotid gland acinar cells, syntaxin-4, SNAP-23 and several other proteins have been identified on plasma membrane (Takuma *et al*., 2000; Imai *et al*., 2004). The specific roles of these proteins in granular secretion have not been determined in detail. However, they may represent specific targets of v-SNAREs on the apical plasma membrane of the acinar cells (Imai *et al*., 2003). The inhibition of cholinergic

parasympathetic innervation at the neuroglandular junction, especially the inhibition of the SNAREs of the acini induced by BoNT, seems to influence the morphological characteristics and secretory functions of the salivary gland.

Another interesting observation of the present study is that the most significant morphological changes occurred in glands treated with both BoNT/A and B. The cleavage of different SNAREs in the presynaptic and acinar cell membrane might be responsible for the more pronounced effects of the combination therapy.

As mentioned above, chemical denervation studies on salivary glands have revealed that no changes occur in amylase secretion (Ellies *et al*., 2004). These findings accord with the acinar changes found in the present study. The development of denervation supersensitivity to secretory agents leads to a greater effect of secretory agents (Emmelin, 1987; Thesleff, 1989). In studies performed in cats, BoNT/A injected into the submandibular gland prevented the release of acetylcholine in salivary glands and produced a supersensitivity towards secretory agents which rose to a high level within 2–3 weeks (Emmelin, 1961). In the absence of nerve-mediated stimuli following parasympathectomy, this increased secretory response may reflect an increased sensitivity to the remaining neural input resulting from an increased number of receptors (Poat and Templeton, 1982; Pazo *et al*., 1989). Further studies are needed to understand the mechanism of action of BoNTs.

Conflict of interest

The authors state no conflict of interest.

References

Ekstrom J, Reinhold AC (2001). Reflex-elicited increases in female rat parotid protein synthesis involving parasympathetic non-adrenergic, non-cholinergic mechanisms. *Exp Physiol* **86**: 605–610.

Ellies M, Gottstein U, Rohrbach-Volland S, Arglebe C, Laskawi R (2004). Reduction of salivary flow with botulinum toxin: extended report on 33 patients with drooling, salivary fistulas, and sialadenitis. *Laryngoscope* **114**: 1856–1860.

Ellies M, Laskawi R, Gotz W, Arglebe C, Tormahlen G (1999). Immunohistochemical and morphometric investigations of the influence of botulinum toxin on the submandibular gland of the rat. *Eur Arch Otorhinolaryngol* **256**: 148–152.

Ellies M, Laskawi R, Rohrbach-Volland S, Arglebe C, Beuche W (2002). Botulinum toxin to reduce saliva flow: selected indications for ultrasound-guided toxin application into salivary glands. *Laryngoscope* **112**: 82–86.

Emmelin N (1961). Supersensitivity of salivary gland caused by botulinum toxin. *J Physiol* **156**: 121–127.

Emmelin N (1987). Nerve interactions in salivary glands. *J Dent Res* **66**: 509–517.

Fujita-Yoshigaki J (1998). Divergence and convergence in regulated exocytosis: the characteristics of cAMP-dependent enzyme secretion of parotid salivary acinar cells. *Cell Signal* **10**: 371–375.

Fujita-Yoshigaki J, Dohke Y, Hara-Yokoyama M, Furuyama S, Sugiya H (1999). Presence of a complex containing vesicle-associated membrane protein 2 in rat parotid acinar cells and its disassembly upon activation of cAMP-dependent protein kinase. *J Biol Chem* **274**: 23642–23646.

Fujita-Yoshigaki J, Dohke Y, Hara-Yokoyama M, Kamata Y, Kozaki S, Furuyama S *et al*. (1996). Vesicle-associated membrane protein 2 is essential for cAMP-regulated exocytosis in rat parotid acinar cells. *J Biol Chem* **271**: 13130–13134.

Garrett JR (1987). The proper role of nerves in salivary secretion: a review. *J Dent Res* **66**: 387–397.

Garrett JR, Suleiman AM, Anderson LC, Proctor GB (1991). Secretory responses in granular ducts and acini of submandibular glands *in vivo* to parasympathetic or sympathetic nerve stimulation in rats. *Cell Tissue Res* **264**: 117–126.

Imai A, Nashida T, Shimomura H (2004). Roles of Munc18-3 in amylase release from rat parotid acinar cells. *Arch Biochem Biophys* **422**: 175–182.

Imai A, Nashida T, Yoshie S, Shimomura H (2003). Intracellular localisation of SNARE proteins in rat parotid acinar cells: SNARE complexes on the apical plasma membrane. *Arch Oral Biol* **48**: 597–604.

Ito S, Karnovsky MJ (1968). Formaldehyde–glutaraldehyde fixatives containing trinitro compounds. *J Cell Biol* **39**: 168A.

Ito S, Winchester RJ (1963). The fine structure of the gastric mucosa in the bat. *J Cell Biol* **16**: 541–577.

Jongerius PH, Rotteveel JJ, van Limbeek J, Gabreels FJ, van Hulst K, van den Hoogen FJ (2004). Botulinum toxin effect on salivary flow rate in children with cerebral palsy. *Neurology* **63**: 1371–1375.

Karnovsky MJ (1971). Use of ferrocyanide-reduced osmium tetroxide in electron microscopy. *J Cell Biol* **51**: 146A.

Lipp A, Trottenberg T, Schink T, Kupsch A, Arnold G (2003). A randomized trial of botulinum toxin A for treatment of drooling. *Neurology* **61**: 1279–1281.

Nashida T, Imai A, Shimomura H (2006). Relation of Rab26 to the amylase release from rat parotid acinar cells. *Arch Oral Biol* **51**: 89–95.

Pazo JH, Rascovsky S, Jerusalinsky D, Medina JH, Tumilasci OR (1989). Increase of muscarinic cholinergic receptors in the rat submandibular glands after parasympathectomy and repeated administration of haloperidol. *Gen Pharmacol* **20**: 759–761.

Poat JA, Templeton D (1982). Non-specific supersensitivity in rat parotid salivary glands following parasympathectomy. *J Auton Pharmacol* **2**: 79–85.

Schneyer CA, Hall HD (1966). Function of rat parotid gland after sympathectomy and total postganglionectomy. *Am J Physiol* **211**: 943–949.

Takuma T, Arakawa T, Tajima Y (2000). Interaction of SNARE proteins in rat parotid acinar cells. *Arch Oral Biol* **45**: 369–375.

Thesleff P (1989). An electrophysiological *in-vivo* study on the effects of nerve stimulation, drugs and denervation in the parotid gland of the rat. *Acta Physiol Scand* **136**: 235–243.

Venable JH, Coggeshall R (1965). A simplified lead citrate stain for use in electron microscopy. *J Cell Biol* **65**: 407–408.

Yoshimura K, Fujita-Yoshigaki J, Murakami M, Segawa A (2002). Cyclic AMP has distinct effects from Ca(2+) in evoking priming and fusion/exocytosis in parotid amylase secretion. *Pflugers Arch* **444**: 586–596.